DeMBA: a developmental atlas for navigating the mouse brain in space and time

Harry Carey[#], Heidi Kleven[#], Martin Øvsthus, Sharon C. Yates, Gergely Csucs, Maja A. Puchades, Jan G. Bjaalie, Trygve B. Leergaard & Ingvild E. Bjerke*

Affiliations:

Neural Systems Laboratory, Institute of Basic Medical Sciences, University of Oslo, Oslo, Norway

* Correspondence: Ingvild E. Bjerke (i.e.bjerke@medisin.uio.no)

Co-first authorship

Key words: reference atlas; postnatal development; mouse brain; spatial registration; data integration

Abstract

Studies of the adult mouse brain have benefited from three-dimensional atlases providing a standard frame of reference for data analysis and integration. Extending these resources to the developing mouse brain has been challenging due to the need to integrate time as a dimension of the atlas. To address this, we present the Developmental Mouse Brain Atlas, a four-dimensional atlas encompassing each postnatal day from 4 to 56.

Main Text

Integration and analysis of mouse brain data depend on three-dimensional common coordinate frameworks[1,2]. Efforts to construct such frameworks have almost exclusively focused on the adult brain, and atlases representing developing brain anatomy have consequently lagged behind. While some studies have addressed this by providing atlases for a subset of discrete, critical developmental stages[3–5], this approach has notable limitations. First, when the temporal dimension is reduced to a subset of stages, data falling between established stages are not represented. Secondly, it fails to represent spatial correspondences across development, making it difficult to integrate and compare data from different ages. Given that one of the fundamental purposes of common coordinate frameworks is to integrate data[1,6,7], the lack of an atlas incorporating time as a continuous dimension is limiting.

To surmount this limitation, we created the Developmental Mouse Brain Atlas (DeMBA), a reference resource with coverage of every postnatal day from 4 to 56 (Figure 1). DeMBA was constructed by using serial two-photon tomography (STPT) templates representing different ages from early postnatal development to adulthood, registering each one to its temporal neighbours and thereby establishing the precise spatial correspondence between each pair. To achieve this, we spatially transformed the Allen Institute Common Coordinate Framework

template (CCFv3[1]; RRID:SCR_020999; postnatal day 56) to developing mouse brain templates (postnatal day 4, 7, 14, 21 and 28) sourced from multiple publicly shared datasets[5,8]. The transformations were based on a three-step (translation, affine, b-spline) registration using elastix[9], optimised by manually defined regions and landmarks. Utilising the resulting spatial transformation matrices, we created interpolated models for the intermediate ages (Figure 1a). The segmentation volumes from the CCFv3 were transformed and interpolated using the same matrices, establishing a four-dimensional (4D) atlas with corresponding regions across postnatal development (Figure 1b-q). The deformation and interpolation was furthermore applied to the developmentally based segmentations provided by the Kim lab[10] (hereafter referred to as the Kim Lab Developmental CCF).

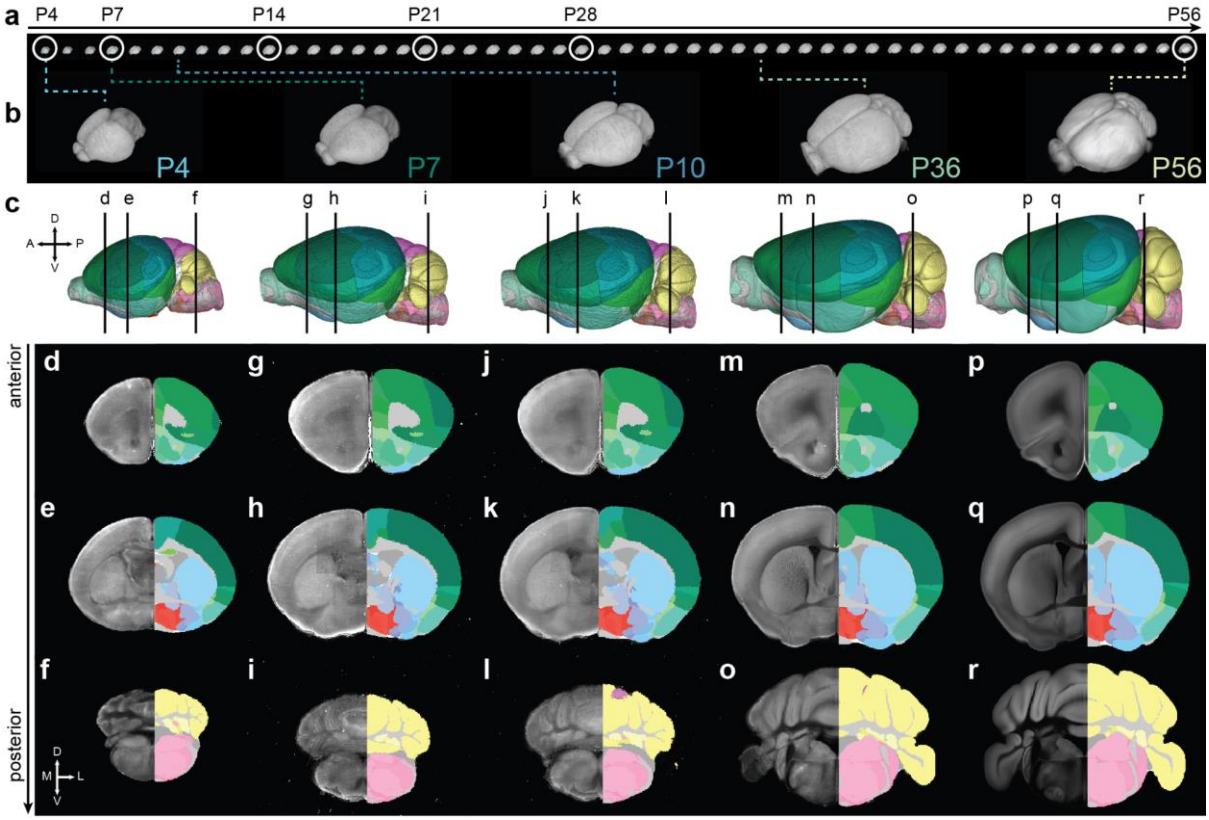

Figure 1. Developmental Mouse brain Atlas with continuous coverage of the postnatal mouse brain. (a) Template volumes from P4 to P56. The ones used for 3D-to-3D registration are indicated with a circle, whereas the remaining ones are interpolated models of intermediate ages. **(b)** Five highlighted template volumes. **(c)** Segmentation volumes from the same ages as highlighted in (b), created by transforming the CCFv3, 2022 segmentation edition to the other

templates. **(d-r)** Coronal sections from three levels across the brain, showing the template (left side) and segmentations (right side) from the same ages as in (b-c).

To facilitate the practical use of DeMBA, we incorporated it in software for spatial registration of brain section images (QuickNII[11]; RRID:SCR_016854; https://quicknii.readthedocs.io/ and VisuAlign[12]; RRID:SCR_017978; https://visualign.readthedocs.io/). This makes DeMBA compatible with the QUINT workflow[13] for quantifying features-of-interest in histological data (Figure 2). To exemplify the use of DeMBA in the QUINT workflow, we analysed calbindin-stained section images from four age groups (P4, P14, P28 and P56; Figure 2a-d) available from the Allen Institute *in situ* hybridization database[14,15]. The images were linearly and non-linearly registered to age-matching DeMBA templates using QuickNII and VisuAlign, respectively. Segmented images (downloaded from the Allen Institute; Figure 2a''-d'') were combined with atlas maps from adult (CCFv3, 2017 edition) and developmental atlas segmentations (Kim Lab Developmental CCF[10]; Figure 2e-h) using an image processing and analysis software (Nutil[16]; RRID:SCR_017183; https://nutil.readthedocs.io). This allowed us to quantify differences in calbindin expression across development based on the segmentations from the two atlases (Figure 2i-j). This use case shows the utility of DeMBA for quantifying features-of-interest in the developing mouse brain.

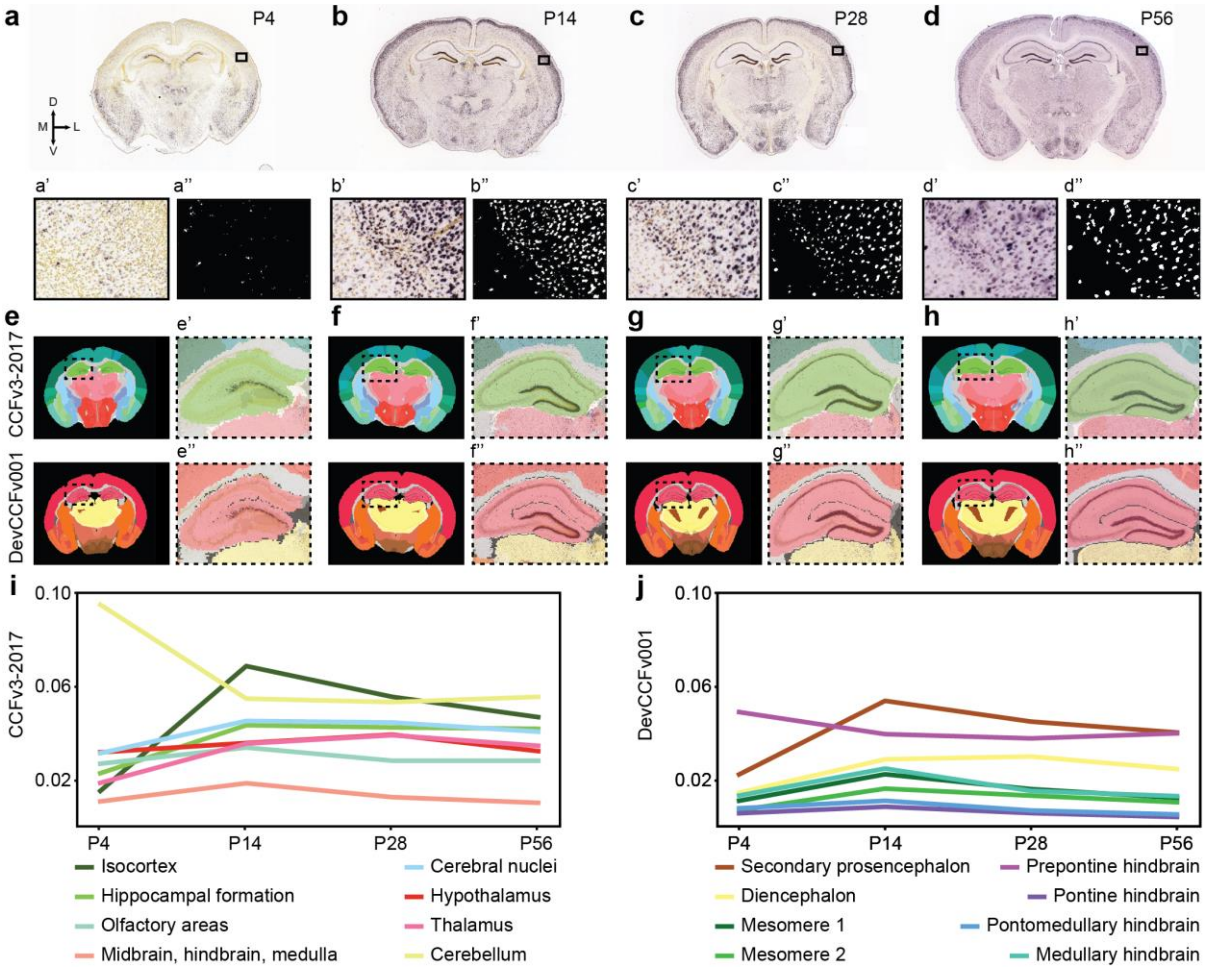

Figure 2. Analysis of brain-wide section data using the QUINT workflow with DeMBA. (a-d) Section images from the Allen Institute *in situ* hybridization database, showing calbindin distribution in four age groups. **(a'-d')** Magnified images from the isocortex. **(a''-d'')** Segmentation images, corresponding to a'-d', used for quantification. **(e-h)** Atlas maps corresponding to the sections in a-d, displaying the adult CCFv3, 2017 segmentation edition (e'-h') and the Kim Lab Developmental CCF (e''-h'') segmentations. **(i-j)** Line graphs showing the calbindin expression load (y axis) across development (x axis), quantified by use of atlas maps from the CCFv3, 2017 (i) and Kim Lab Developmental CCF (j).

DeMBA builds on and advances recent efforts to develop methods for transforming developmental mouse brain data between ages[17], and interpolating between templates[18,19]. DeMBA is the first atlas to combine time as a continuous variable with detailed segmentations and user-friendly software for spatial registration and comparative analyses. A further benefit of DeMBA is that any segmentation volume or reference template registered to the CCFv3 can be transformed to any age using the transformation matrices defined through the creation of

the atlas (as exemplified with the Kim Lab Developmental CCF; Figure 2), thus making resources for the adult available for the developing brain.

To summarise, DeMBA is a 4D atlas, with time represented as a continuous dimension, providing a dynamic representation of the developing brain. It was established based on spatial transformation of the most widely used common coordinate framework for the adult mouse brain to templates from different postnatal ages. Incorporated in user-friendly software, DeMBA can be used for spatiotemporal analysis and interpolation of templates and data to intermediate ages. We envision this atlas and associated software will allow researchers to substantially improve the accuracy and efficiency of developing mouse brain studies.

Methods

To fit the brain region delineations from the Allen Mouse brain Common Coordinate Framework to each of the developing mouse brain templates, we used elastix to perform an automated, nonlinear registration. To improve the transformations, we used manually defined corresponding landmarks or regions in each pair of template volumes. The quality of the transformation was assessed using a set of expert-defined landmarks independent from those used in the registration. We then interpolated the transformations, creating models for every postnatal day in between the ages with existing templates. Lastly, we implemented the atlas in the suite of software of the QUINT workflow. In the following, we first describe the reference template and segmentation files, before outlining the methodology for each procedure: 3D-to-3D registration, validation, interpolation and implementation in software.

Reference template and segmentation files

Allen Common Coordinate Framework reference template and segmentations. We used the Allen mouse brain Common Coordinate Framework template (CCFv3[1]) at 10 µm isotropic resolution. This template is a population-averaged serial two-photon tomography template based on 1675 subjects. We further used the 2017 and 2022 editions of the segmentation volume, both at a 10 µm resolution. The two segmentation volumes differ in the amount of annotated brain regions, with the most recent edition having more detailed annotations in the hippocampus and olfactory bulb. The template and segmentations are available from the Allen Institute archive (https://download.alleninstitute.org/informatics-archive/current-release/mouse_ccf). To match the resolution and dimensions of the developmental reference templates (see below), we downsampled the template and segmentation volumes from the Allen Institute to 20 µm and padded the posterior end of the volume with 45 extra voxels.

Developmental reference templates. We used the serial two-photon tomography volumes provided in the supplementary material of the publication by Newmaster and colleagues[8]. These files were shared as one .tif file for each age (P7, P14, P21, and P28). The original volumes had non-isotropic voxels with a 20 × 20 × 50 µm resolution. We resampled them to isotropic 20 × 20 × 20 µm voxel size using AMIRA (version 6.3.0; https://www.thermofisher.com/no/en/home/electron-microscopy/products/software-em-3d-vis/amira-software.html). We also used the P4 volume shared by Liwang and colleagues[5], which was provided as a .tif file with isotropic 20 × 20 × 20 µm voxel size. All volumes were converted to .nii.gz files for further processing.

To optimise the developmental reference templates for successive co-registration and use in neuroinformatics software, we implemented several preprocessing steps. First, we removed a slight tilt around the mediolateral axis in template P7, P14, P21 and 28, ensuring they were as symmetric as possible. Secondly, we determined the Waxholm Space origin[20] for all the templates and aligned them with the corresponding position in the adult mouse brain CCFv3. Next, we standardised the dimensions of the templates as they had a longer rostrocaudal dimension than the adult CCFv3. To amend this, we cropped some rostrally situated voxels outside the brain in the developmental reference templates. However, cropping voxels in the caudal part would affect voxels representing the brain, and we therefore resolved this by adding voxels in the caudal part of the adult CCFv3 template (see section above). We furthermore adjusted the brightness and sharpness of the templates, and adjusted the histograms to the same mean intensity value. The developmental reference templates, including detailed information about each pre-processing step, are available through the EBRAINS research infrastructure[21–25] (RRID:SCR_019260; https://ebrains.eu/).

3D-to-3D registration using elastix

Prior to the 3D-to-3D registration, we applied a Contrast Limited Adaptive Histogram Equalization (CLAHE) filter[26] to enhance the contrast in the templates. To perform registration of the CCFv3 template to each developmental reference template, we used the SimpleITK python package (https://simpleelastix.readthedocs.io/) and elastix[9] (RRID:SCR_009619; https://elastix.lumc.nl/). We performed a three-step (translation, affine and b-spline) registration, with the b-spline registration using pairs of manually defined, corresponding landmarks or regions in the two templates to optimise the registration.

To define corresponding regions across templates, we used a combination of manual and automatic segmentation in ITK-snap[27] (http://www.itksnap.org/). Defining corresponding regions were only used in cases where a region showed overall poor fit, and the use of a single point to improve it was infeasible, e.g. for the granular cell layer of the dentate gyrus.

Corresponding landmarks were defined using ITK-snap. We experienced that the addition of many manually defined landmarks made the registration overall worse. Even when these landmarks were rigorously defined in terms of anatomical correspondence, they did not necessarily aid the registration when they were positioned in areas where the automatic procedure already performed well. We therefore opted to add individual landmarks on a need-to-improve basis and evaluating the result of adding individual landmark after running the registration. As a first step, we ran the automatic registration with no landmarks added, and the result of this was used as a baseline upon which we gradually refined the registration by adding landmarks in areas where the registration was deemed suboptimal.

We performed an age-to-age registration, where the registration for each template was performed by use of the template closest to its age. The challenge with this approach was that

errors in the transformation will propagate down through subsequent registrations. To avoid this, we used the transformed template from the previous registration for each new registration, as this template would have perfect correspondence with the transformed segmentations. The exception was the P28-P21 registration (adult CCFv3 template warped to P28). Because of the differences in acquisition between the adult CCFv3 and the developmental reference templates, the benefit of not propagating small errors was outweighed by the challenges caused by the relatively dissimilar appearance of the transformed adult template. Thus, the adult CCFv3 was first transformed to the P28 template. Then, the P28 template was registered to the P21 template. The volume resulting from transforming the P28 template to P21 was used in the subsequent registration to the P14 template, and so on, until the lowest age (P4) was reached. For each registration, we used the general procedure of gradual refinement by use of landmarks described above; the exact landmarks used, and challenges resolved in each registration therefore differed across the age groups. Detailed information about each registration, including information about parameters and landmarks or regions used, are available on the EBRAINS Knowledge Graph[28–32] (RRID:SCR_017612; https://search.kg.ebrains.eu/).

Interpolation of transformation and application to segmentations

To create models for ages between the developmental reference templates (P4, P7, P14, P21, P28 and P56), we interpolated the transformation matrices. First, the transformation information from elastix was used to calculate the transformation matrix for each registration, here referred to as the *backwards* transformation matrix. This matrix was inverted to create the *forwards* transformation matrix. The forwards and backwards transformation matrices were then applied to each template volume, except for the P56 (where only the backwards transformation matrix was applied) and the P4 (where only the forwards transformation matrix was applied). Since the segmentations were being transformed down from the adult template

and not vice versa, only the backwards transformation matrix was applied to the segmentation volumes. Adjusting the magnitude of each transformation matrix allowed us to create models of the intermediate ages. For each postnatal day, the models resulting from the forwards and backwards transformation was averaged to arrive at a final model. Lastly, the templates and models for every day from P4 to P56 were combined into a compiled volume with time as a dimension. To keep the file size of this compiled volume manageable, we split it into two volumes representing the first (P4-P29) and second (P30-P56) half of the age range. Detailed information is available on the EBRAINS Knowledge Graph[33].

Implementation in software

To facilitate the use of the DeMBA atlas in integration and analysis of data from the developing mouse brain, we implemented the atlas in the suite of software of the QUINT workflow[13]. This includes the QuickNII software[11] for linear registration of histological sections to 3D reference atlases an VisuAlign[12], which allows non-linear refinement of QuickNII registrations. DeMBA can be used with the Nutil software[16] through the custom atlas function, allowing quantification of features across the brain. The QuickNII software has so far been provided with separate versions for different atlas volumes; a non-optimal solution for the DeMBA atlas which consists of 53 volumes. We therefore implemented all the DeMBA volumes in a single QuickNII package, and added a pop-up window where the user can select which postnatal day of the atlas to launch. We also implemented DeMBA in VisuAlign with separate packages for the adult and the developmental segmentation volumes (CCFv3, 2017 edition; CCFv3, 2022 edition[1]; Kim Lab Developmental CCF[10]). VisuAlign will automatically open the atlas to which the data were QuickNII-registered when the user selects a file. The new versions of the software were shared through the EBRAINS Knowledge Graph (https://search.kg.ebrains.eu).

Example use of DeMBA with the QUINT workflow

To exemplify the use of DeMBA in the QUINT workflow, we analysed calbindin-stained serial sections from four brains (aged P4, P14, P28 and P56), accessed via the Allen Institute *in situ* hybridization database[14,15]. The selected series included experiment IDs 100059245 (P4), 100045313 (P14), 100045526 (P28), and 71717640 (P56). Both raw images and corresponding segmented images for each series were downloaded. We registered the images to age-matched DeMBA templates using QuickNII (v2.2) and refined the registration using VisuAlign (v0.9). Atlas maps were exported for both adult (CCFv3, 2017 edition) and developmental (Kim Lab Developmental CCF, v001) segmentations and combined with the segmented images using Nutil (v0.8.0). The custom atlas feature was used to enable quantification of calbindin-expressing neurons with DeMBA. We analysed the load of calbindin expression in major brain regions, excluding white matter tracts and ventricles, with the adult and the developmental segmentation.

Data and Code Availability

All the code used in this study is available from the DeMBA Github repository (https://github.com/ingvildeb/DeMBA_scripts), and all the datasets are available via the EBRAINS research infrastructure (https://search.kg.ebrains.eu/?category=Dataset#904b7981-0c68-4af6-b3bb-3d9a648b3a7c).

The developmental reference templates are available from the following datasets on the EBRAINS Knowledge Graph:

- Carey, H., Kleven, H., Leergaard, T. B., & Bjerke, I. E. (2024). Population-averaged 3D isotropic serial two-photon tomography reference data for the P4 mouse brain (v1) [Data set]. EBRAINS. doi:10.25493/VNF6-E92
- Carey, H., Kleven, H., Qu, H., Leergaard, T. B., & Bjerke, I. E. (2024). Population-averaged 3D isotropic serial two-photon tomography reference data for the P7 mouse brain (v2) [Data set]. EBRAINS. doi:10.25493/JKBM-608
- Carey, H., Kleven, H., Qu, H., Leergaard, T. B., & Bjerke, I. E. (2024). Population-averaged 3D isotropic serial two-photon tomography reference data for the P14 mouse brain (v2) [Data set]. EBRAINS. doi:10.25493/KAHK-14
- Carey, H., Kleven, H., Qu, H., Leergaard, T. B., & Bjerke, I. E. (2024). Population-averaged 3D isotropic serial two-photon tomography reference data for the P21 mouse brain (v2) [Data set]. EBRAINS. doi:10.25493/2FMJ-152
- Carey, H., Kleven, H., Qu, H., Leergaard, T. B., & Bjerke, I. E. (2024). Population-averaged 3D isotropic serial two-photon tomography reference data for the P28 mouse brain (v2) [Data set]. EBRAINS. doi:10.25493/TG8Z-PER

All the data related to the transformation between the templates are available from the following datasets:

- Carey, H., Ovsthus, M., Kleven, H., Leergaard, T. B., & Bjerke, I. E. (2024). Allen Mouse Brain CCFv3 segmentations transformed to P4 population-averaged serial two-photon tomography data (v1) [Data set]. EBRAINS. doi:10.25493/QG9H-16Y
- Ovsthus, M., Carey, H., Kleven, H., Leergaard, T. B., & Bjerke, I. E. (2024). Allen Mouse Brain CCFv3 segmentations transformed to P7 population-averaged serial two-photon tomography data (v1) [Data set]. EBRAINS. doi:10.25493/NAWP-ND2
- Ovsthus, M., Carey, H., Kleven, H., Leergaard, T. B., & Bjerke, I. E. (2024). Allen Mouse Brain CCFv3 segmentations transformed to P14 population-averaged serial two-photon tomography data (v1) [Data set]. EBRAINS. doi:10.25493/SZSR-BFZ
- Ovsthus, M., Carey, H., Kleven, H., Leergaard, T. B., & Bjerke, I. E. (2024). Allen Mouse Brain CCFv3 segmentations transformed to P21 population-averaged serial two-photon tomography data (v1) [Data set]. EBRAINS. doi:10.25493/JZKH-XWK
- Ovsthus, M., Carey, H., Kleven, H., Leergaard, T. B., & Bjerke, I. E. (2024). Allen Mouse Brain CCFv3 segmentations transformed to P28 population-averaged serial two-photon tomography data (v1) [Data set]. EBRAINS. doi:10.25493/GVT5-4K9

The DeMBA, including developmental reference templates, models and segmentations, and the software incorporating DeMBA, are available from the following dataset:

- Carey, H., Ovsthus, M., Kleven, H., Yates, S. C., Csucs, G., Puchades M. A., Bjaalie, J. G., Leergaard, T. B., & Bjerke, I. E. (2024). Developmental mouse brain atlas (DeMBA) with continuous coverage of postnatal day 4 to 56 (v1) [Data set]. EBRAINS. doi:10.25493/PWDG-536

Acknowledgements

This work received funding from European Union's Horizon 2020 Framework Program for Research and Innovation under the specific grant agreement no. 945539 (Human Brain Project SGA3); the European Union's Research and Innovation Program Horizon Europe under Grant Agreement no. 101147319 (EBRAINS 2.0); and UNIFOR-FRIMED.

References

1. Wang, Q. *et al.* The Allen Mouse Brain Common Coordinate Framework: A 3D reference atlas. *Cell* **181**, 1–18 (2020).

2. Leergaard, T. & Bjaalie, J. Atlas-based data integration for mapping the connections and architecture of the brain. *Science (80-.).* **378**, 488–492 (2022).

3. Kronman, F. *et al.* Developmental Mouse Brain Common Coordinate Framework. *bioRxiv* (2023).

4. Riffault, B. *et al.* A quantitative cholinergic and catecholaminergic 3D Atlas of the developing mouse brain. *Neuroimage* **260**, 119494 (2022).

5. Liwang, J. *et al.* epDevAtlas: Mapping GABAergic cells and microglia in postnatal mouse brains. *bioRxiv* (2023).

6. Bjerke, I. *et al.* Data integration through brain atlasing: Human Brain Project tools and strategies. *Eur. Psychiatry* **50**, 70–76 (2018).

7. Kleven, H. *et al.* Waxholm Space atlas of the rat brain: a 3D atlas supporting data analysis and integration. *Nat. Methods* 1–25 (2023) doi:10.1038/s41592-023-02034-3.

8. Newmaster, K. *et al.* Quantitative cellular-resolution map of the oxytocin receptor in postnatally developing mouse brains. *Nat. Commun.* **11**, 1–12 (2020).

9. Klein, S., Staring, M., Murphy, K., Viergever, M. A. & Pluim, J. P. W. Elastix: A toolbox for intensity-based medical image registration. *IEEE Trans. Med. Imaging* **29**, 196–205 (2010).

10. Kim, Y. KimLabDevCCFv001. *Mendeley Data* (2022) doi:10.17632/2svx788ddf.1.

11. Puchades, M., Csucs, G., Ledergerber, D., Leergaard, T. & Bjaalie, J. Spatial registration of serial microscopic brain images to three-dimensional reference atlases with the QuickNII tool. *PLoS One* **14**, e0216796 (2019).

12. Gurdon, B. *et al.* Detecting the effect of genetic diversity on brain composition in an Alzheimer's disease mouse model. *Commun. Biol.* **7**, 605 (2024).

13. Yates, S. *et al.* QUINT: Workflow for Quantification and Spatial Analysis of Features in Histological Images From Rodent Brain. *Front. Neuroinform.* **13**, 1–14 (2019).

14. Lein, E. *et al.* Genome-wide atlas of gene expression in the adult mouse brain. *Nature* **445**, 168–176 (2007).

15. Thompson, C. *et al.* A High-Resolution Spatiotemporal Atlas of Gene Expression of the Developing Mouse Brain. *Neuron* **83**, 309–323 (2014).

16. Groeneboom, N., Yates, S., Puchades, M. & Bjaalie, J. Nutil: A Pre- and Post-processing Toolbox for Histological Rodent Brain Section Images. *Front. Neuroinform.* **14**, 37 (2020).

17. Wu, D. *et al.* A diffusion MRI-based spatiotemporal continuum of the embryonic mouse brain for probing gene–neuroanatomy connections. *Proc. Natl. Acad. Sci.* **119**, e2111869119 (2022).

18. Szulc, K. *et al.* 4D MEMRI atlas of neonatal FVB/N mouse brain development. *Neuroimage* **118**, 49–62 (2015).

19. Tustison, N. *et al.* The ANTsX Ecosystem for Mapping the Mouse Brain. *bioRxiv* (2024).

20. Johnson, G. *et al.* Waxholm Space: An image-based reference for coordinating mouse

brain research. *Neuroimage* **53**, 365–372 (2010).

21. Carey, H., Kleven, H., Leergaard, T. & Bjerke, I. Population-averaged 3D isotropic serial two-photon tomography reference data for the P4 mouse brain (v1). at https://doi.org/10.25493/VNF6-E92 (2024).

22. Carey, H., Kleven, H., Qu, H., Leergaard, T. & Bjerke, I. Population-averaged 3D isotropic serial two-photon tomography reference data for the P7 mouse brain (v2). at https://doi.org/10.25493/JKBM-608 (2024).

23. Carey, H., Kleven, H., Qu, H., Leergaard, T. & Bjerke, I. Population-averaged 3D isotropic serial two-photon tomography reference data for the P14 mouse brain (v2). at https://doi.org/10.25493/KAHK-14 (2024).

24. Carey, H., Kleven, H., Qu, H., Leergaard, T. & Bjerke, I. Population-averaged 3D isotropic serial two-photon tomography reference data for the P21 mouse brain (v2). at https://doi.org/10.25493/2FMJ-152 (2024).

25. Carey, H., Kleven, H., Qu, H., Leergaard, T. & Bjerke, I. Population-averaged 3D isotropic serial two-photon tomography reference data for the P28 mouse brain (v2). at https://doi.org/10.25493/TG8Z-PER (2024).

26. Pizer, S. M. *et al.* Adaptive Histogram Equalization and Its Variations. *Comput. VISION, Graph. IMAGE Process.* **39**, 355–368 (1987).

27. Yushkevich, P. *et al.* User-guided 3D active contour segmentation of anatomical structures: Significantly improved efficiency and reliability. *Neuroimage* **31**, 1116–1128 (2006).

28. Carey, H., Ovsthus, M., Kleven, H., Leergaard, T. & Bjerke, I. Allen Mouse Brain

CCFv3 segmentations transformed to P4 population-averaged serial two-photon tomography data (v1). at https://doi.org/10.25493/QG9H-16Y (2024).

29. Ovsthus, M., Carey, H., Kleven, H., Leergaard, T. & Bjerke, I. Allen Mouse Brain CCFv3 segmentations transformed to P7 population-averaged serial two-photon tomography data (v1). at https://doi.org/10.25493/NAWP-ND2 (2024).

30. Ovsthus, M., Carey, H., Kleven, H., Leergaard, T. & Bjerke, I. Allen Mouse Brain CCFv3 segmentations transformed to P14 population-averaged serial two-photon tomography data (v1). at https://doi.org/10.25493/SZSR-BFZ (2024).

31. Ovsthus, M., Carey, H., Kleven, H., Leergaard, T. & Bjerke, I. Allen Mouse Brain CCFv3 segmentations transformed to P21 population-averaged serial two-photon tomography data (v1). at https://doi.org/10.25493/JZKH-XWK (2024).

32. Ovsthus, M., Carey, H., Kleven, H., Leergaard, T. & Bjerke, I. Allen Mouse Brain CCFv3 segmentations transformed to P28 population-averaged serial two-photon tomography data (v1). at https://doi.org/10.25493/GVT5-4K9 (2024).

33. Carey, H. *et al.* Developmental mouse brain atlas (DeMBA) with continuous coverage of postnatal day 4 to 56 (v1). at https://doi.org/10.25493/PWDG-536 (2024).